



Peripheral quantitative computed tomography (pQCT)–based finite element analysis provides enhanced diagnostic performance in identifying non-vertebral fracture patients compared with dual-energy X-ray absorptiometry

H. Jiang¹ · D.L. Robinson² · C.J. Yates^{1,3,4} · P.V.S. Lee² · J.D. Wark^{1,3,4}

Received: 5 May 2019 / Accepted: 28 October 2019 / Published online: 13 November 2019
© International Osteoporosis Foundation and National Osteoporosis Foundation 2019

Abstract

Summary Due to limitations of the predominant clinical method for diagnosing osteoporosis, an engineering model based on a dedicated CT scanner for bone density and structure was applied in fracture patients and controls. Improved diagnostic performance was observed, which supports its potential use in future research and clinical practice.

Introduction Dual-energy X-ray absorptiometry (DXA), the predominant clinical method for diagnosing osteoporosis, has limitations in identifying individuals with increased fracture risk. Peripheral quantitative computed tomography (pQCT) provides additional information and can be used to generate finite element (FE) models from which bone strength properties can be estimated. We investigated the ability of pQCT-FE properties to distinguish peripheral low-trauma fracture patients from healthy controls, by comparison with DXA and standard pQCT.

Methods One hundred and eight fracture patients (77 females aged 67.7 ± 7.9 years, 31 males aged 69.7 ± 8.9 years) were recruited from a hospital fracture liaison service. One hundred and twenty healthy community controls (85 females aged 69.8 ± 8.5 years, 35 males aged 68.9 ± 7.2 years) were recruited.

Results Significant differences between groups were observed in pQCT-FE properties, especially at the 4% tibia site. Fracture odds increased most per standard deviation decrease in pQCT-FE at this location [shear stiffness estimate, k_{shear} in females, OR = 10.34, 95% CI (1.91, 43.98); bending stiffness estimate, k_{bend} in males, OR = 8.32, 95% CI (4.15, 33.84)]. Area under the receiver operating characteristics curve (AUROC) was observed to be highest with pQCT-FE properties at 4% the tibia site. In females, this was 0.83 for the pQCT-FE variable k_{shear} , compared with 0.72 for DXA total hip bone density (TH aBMD) and 0.76 for pQCT tibia trabecular density (Trb vBMD); in males, this was 0.81 for the pQCT-FE variable k_{bend} at the 4% tibia site, compared with 0.62 for TH aBMD and 0.71 for Trb vBMD. There were significant differences in AUROC between DXA and pQCT-FE variables in both females ($p = 0.02$) and males ($p = 0.03$), while no difference was observed in AUROC between primary pQCT and pQCT-FE variables.

Conclusions pQCT-FE modeling can provide enhanced diagnostic performance compared with DXA and, given its moderate cost, may be useful in clinical settings.

Keywords AUROC · bone strength · fracture status · finite element modeling · pQCT

Electronic supplementary material The online version of this article (<https://doi.org/10.1007/s00198-019-05213-1>) contains supplementary material, which is available to authorized users.

✉ J.D. Wark
jdwork@unimelb.edu.au

¹ Department of Medicine, Royal Melbourne Hospital, University of Melbourne, Melbourne, Victoria 3052, Australia

² Department of Biomedical Engineering, University of Melbourne, Melbourne 3052, Victoria, Australia

³ Bone and Mineral Medicine, Royal Melbourne Hospital, Melbourne 3052, Victoria, Australia

⁴ Department of Diabetes and Endocrinology, Royal Melbourne Hospital, Melbourne 3052, Victoria, Australia

Introduction

The prevalence of osteoporosis is increasing due to population ageing worldwide [1]. Being a “silent” disease, osteoporosis may not attract the attention of patients and primary healthcare practitioners until a fragility fracture occurs. It has been estimated that one-third of women and one-fifth of men will sustain a fragility fracture after age 50 years [2], which is a great societal burden associated with high morbidity, mortality and healthcare expenditure. Although many modifiable risk factors for bone fragility have been identified previously, better screening, case-finding and monitoring strategies are still needed given the intrinsic limitations of dual-energy X-ray absorptiometry (DXA) [3].

Although DXA is considered the clinical criterion method for osteoporosis diagnosis, almost seventy percent of patients who had recently sustained a low-trauma fracture were diagnosed with osteopenia or normal bone density based on DXA measurements at our institution [4]. This misclassification is due in part to the technique itself which projects the region of interest into a two-dimensional plane. This data acquisition from a projective X-ray technique does not take bone “depth” into account, thus making results susceptible to artefacts related to different bone sizes. DXA also fails to capture other bone geometric information including cortical thickness which has been closely correlated to bone fragility [5]. In addition, DXA is performed routinely at central sites, i.e. the lumbar spine and the proximal femur in clinical practice, while a large proportion of fragility fractures occur at more peripheral sites, e.g. the distal forearm [2], where fracture is an early indication of bone fragility [6].

Peripheral quantitative computed tomography (pQCT) provides both volumetric bone density and bone geometry measurements which correlate well with bone mechanical properties at multiple peripheral sites [7–9]. These variables can differentiate between people with and without prevalent fractures [10] and are associated with fracture occurrence during follow-up in both women and men [11, 12]. Therefore, pQCT has a potential role in improving our understanding of bone fragility compared to using DXA alone [4]. Finite element (FE) analysis is a computational method that can provide non-invasive assessment of bone strength in vivo. FE models based on quantitative computed tomography (QCT) images of either the vertebral body or the proximal femur have provided estimates of bone strength that correlate strongly with cadaveric fracture loads [13, 14], and these correlations were reported to be higher than those of bone mineral density (BMD) measured by DXA [13, 15]. FE models of cadaveric forearm or tibia using either QCT or pQCT were established previously [16–18]. While these studies showed good correlation between FE properties and fracture failure load, the models were time-consuming to build and imparted considerable radiation to image the entire bone or joint, thus limiting their use in

clinical settings. Since it is designed for measurement at the appendicular skeleton, pQCT is a potentially suitable source for FE analysis at peripheral sites with its volumetric data acquisition, spatial distribution of bone density and comparable resolution with QCT. Moreover, pQCT instruments can be acquired and operated at quite moderate cost.

In this current study, we aimed to evaluate the ability of a clinically relevant, pQCT-based FE model (pQCT-FE) to estimate bone strength in patients with recent fragility fractures and age-matched controls and to compare the diagnostic characteristics of DXA, pQCT and pQCT-FE variables.

Methods

Participants

Two groups of participants were recruited for this study. The fracture group was recruited from a fracture liaison service involving multiple disciplines at a tertiary hospital, which improves uptake of osteoporosis intervention guidelines in a cost-effective way [19]. The control group was recruited through electronic and paper-based advertisements from multiple sources, including members of a community education program (University of the Third Age), staff, volunteers, visitors and contacts of the University of Melbourne and the Royal Melbourne Hospital.

General inclusion criteria for both groups were as follows: [1] aged 50 years or above, [2] English-speaking or has an English-speaking family member or friend available, [3] consent to participate in this study and be able to attend a study visit at the Royal Melbourne Hospital. Specific inclusion criteria for the fracture group were as follows: [1] had sustained at least one low-trauma fracture, i.e. a fracture caused by minimal trauma such as a fall from a standing height or less, within 3 months prior to a study visit; [2] for patients with two or more fractures, there were at least one radius and one tibia without a fracture history or other relevant pathology and available for measurement. Specific inclusion criterion for the control group was as follows: reported no prior history of osteoporosis, low bone density or low-trauma fracture.

General exclusion criteria for both groups were as follows: [1] prior diagnosis of osteoporosis; [2] prolonged (> 3 months) use of osteoporosis therapy, including bisphosphonates, denosumab, selective oestrogen receptor modulators and hormone replacement therapy in the past 2 years; [3] prior therapy with teriparatide or strontium ranelate; [4] other medical conditions which may affect bone health, e.g. hyperthyroidism, hyperparathyroidism, Crohn’s disease, diabetes and Cushing syndrome; [5] currently taking or have recently taken medications which may affect bone health, e.g. glucocorticoid agents, anti-epilepsy drugs and heparin.

DXA scanning and analysis protocol

Standard clinical scans of the lumbar spine (L1–L4) and the right hip were performed using a fan-beam densitometer (Horizon QDR 4500A, Hologic Inc., Bedford, MA, USA). In cases where participants had a right-sided hip replacement or fracture, the left hip was scanned. DXA scans were performed in array mode and were analysed using the manufacturer's commercial software (v 9.10D). Variables of interest included areal bone mineral density (aBMD) of the lumbar spine (LS aBMD), the total hip (TH aBMD) and the femoral neck (FN aBMD). The 12-month precision of the scanner for the Hologic spine phantom was 0.39% for aBMD.

pQCT scanning and analysis protocol

Scans of the non-dominant radius and tibia were performed using an XCT 3000 pQCT scanner (Stratec Medizintechnik, Pforzheim, Germany) at both the 4% and 66% sites along the limb length. Length was measured from the ulna styloid process to the olecranon process at the forearm and from the base of the medial malleolus to the superior margin of the medial condyle at the tibia. In fracture patients whose non-dominant radius/tibia sustained a fracture, the dominant side was scanned. A scout scan was performed to identify the correct starting line, which was taken as the distal articular surface of the radius or tibia. A single slice at each site was acquired with an in-plane resolution of 0.4×0.4 mm and a slice thickness of 2 mm. Scanning speed was 10 mm/s. The manufacturer's commercial software (version XCT 5.50E) was used to analyse pQCT images for standard pQCT variables. Variables of interest included total volumetric bone mineral density (Tot vBMD), trabecular volumetric bone mineral density (Trb vBMD) and trabecular cross-sectional area (Trb CSA) at the 4% site and cortical volumetric bone mineral density (Crt vBMD), cortical thickness (Crt Thk) and polar stress-strain index (SSI_p) at the 66% site.

FE model properties

Detailed methodology of the pQCT-FE models was described elsewhere [20]. Briefly, all pQCT images were exported to MATLAB (version R2016b, Mathworks, Natick, MA, USA), where manual segmentation was performed. A mesh of $0.4 \times 0.4 \times 2$ mm elements was generated from segmentation and then re-sliced in the z -direction to produce a mesh of $0.4 \times 0.4 \times 0.4$ mm elements. The Young's modulus was calculated using an established equation for the tibia [21] and the radius [18] and was assigned to each element. Each voxel mesh was then used to generate a FE model in Abaqus (version 6.11, Simulia, Dassault Systems, Providence, RI, USA).

Four loading cases were considered for all FE Models (Fig. 1): axial compression, shear, bending and torsion. Axial compression was simulated by a 0.01-mm displacement of the superior surface towards the inferior surface (Fig. 1a). Shear was simulated by a 0.01-mm displacement of the superior surface in the direction of either the x - or y -axes (Fig. 1b). Bending was simulated by a 0.0001 radian rotation of the inferior surface about either the x - or y -axes (i.e. cross-section neutral axes; Fig. 1c). Torsion was simulated by a 0.0001 radian rotation of the inferior surface about the z -axis (Fig. 1d). The reaction forces and moments predicted from the simulations were divided by the respective applied displacement or rotation to derive the compressive, shear, bending and torsional stiffness (k_{comp} , k_{shear} , k_{bend} and k_{torsion} , respectively) of each cross section. The bending and shear stiffness were each taken as the minimum value derived from the two neutral axis directions.

Other data collected

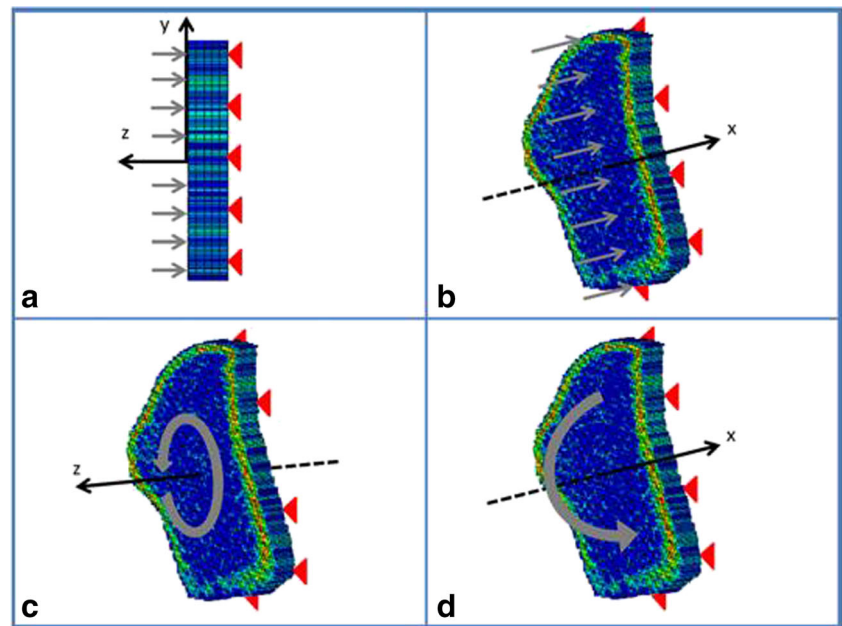
An ethics-approved questionnaire was used to collect other information from participants. The information included date of birth, sex, height, weight, fracture details/history, comorbidities, related medical history and risk factors for osteoporotic fracture according to the FRAX® algorithm (<https://www.sheffield.ac.uk/FRAX>).

Statistical analysis

Descriptive statistics were expressed as mean \pm 1.0 standard deviation (SD). Difference between groups was assessed using a two-sample t test for variables that were normally distributed or the Kolmogorov-Smirnov test for variables that were not normally distributed. Multivariate linear regression models were established to compare means between groups while adjusting for age, height and weight. To identify multicollinearity between variables, multivariate linear regression models were established for each group of variables including DXA, pQCT radius/tibia and pQCT-FE stiffness of 4/66% radius/tibia, from which variance inflation factors (VIFs) were derived for each variable. Age, height and weight were included in each model. Collinearity was assumed with a VIF > 5 [22].

For all DXA variables, and pQCT and pQCT-FE variables that varied significantly between the control and fracture groups, a binary logistic regression was established to evaluate their relationship with fracture status. All logistic regression models were adjusted for confounding factors including age, height and weight. Results of logistic regression models were expressed as odds ratio (OR) per SD decrease of the respective variable and its 95% confidence interval (95% CI). In the case of variables determined to be collinear

Fig. 1 Loading cases of pQCT-FE. Figures show examples of 4% radius. **a** Axial compression loading case. Grey arrows applied displacement of 0.01 mm in the negative z direction. **b** Shear loading case. Grey arrows applied displacement of 0.01 mm in either positive x direction or positive y direction. **c** Torsion loading case. Grey arrow applied rotation of 0.0001 radians about z -axis. **d** Bending loading case. Grey arrow applied rotation of 0.0001 radians about either x - or y -axis.



according to the VIFs, only the variable with the highest average OR was included in the analysis.

Specificity, sensitivity and area under the receiver operating characteristics (AUROC) curve were obtained from the logistic regression models to show the ability of each predictor to classify between fracture patients and controls. The significance of differences between the AUROCs of key DXA, pQCT and pQCT-FE variables (i.e. those with highest AUROC value in each group of DXA, standard pQCT and pQCT-FE variables) was determined using the method by Delong et al [23], which is a non-parametric method based on U -statistics from which the test statistic follows a χ^2 distribution. All statistical analyses were performed in SPSS (version 25, SPSS Inc., Chicago, IL, USA). All significance levels were set as $p < 0.05$.

Results

One hundred and eight fracture patients (77 females, 31 males) and 120 controls (85 females, 35 males) were recruited into this study (Table 1). No significant difference was observed in age, height, weight, BMI, sex or radius/tibia length between the fracture patients and controls. Among fracture risk factors, no difference between groups was observed in alcohol consumption. The fracture group had a higher rate of smoking than the control group ($p = 0.01$). More fracture patients were found to have rheumatoid arthritis than controls ($p = 0.03$), and their parental hip fracture incidence was also greater ($p = 0.01$). For fracture patients, the average interval between fracture and the study visit (mean \pm SD) was 56.6 \pm 13.2 days. Most fractures sustained were non-vertebral.

Colles' fractures accounted for the major proportion of all fractures (60.7%), followed by lower leg (13.9%) and humerus (9.0%) fractures (Table 1).

A difference between the fracture group and the control group was observed in TH aBMD but not in DXA aBMD variables at other sites; however, the difference was not significant after adjustment for age, height, weight and sex (Table 2). Several standard pQCT variables differed between groups before adjustment for age, height, weight and sex, but the only variables with significant difference between groups after adjustment were Trb vBMD at both the radius and the tibia ($p = 0.01$ and 0.02 for the radius and the tibia, respectively). No pQCT-FE variables differed between groups at the 4% radius site. At the 66% radius site, k_{comp} and k_{bend} were lower in the fracture patients than in the controls after adjustment for age, height, weight and sex ($p = 0.04$ and 0.03, respectively). At the 4% tibia site, all pQCT-FE variables differed between groups before adjustment for age, height, weight and sex, although the differences were not statistically significant for k_{bend} and k_{torsion} after adjustment for age, height, weight and sex. At the 66% tibia site, all pQCT-FE stiffness variables except k_{torsion} differed between groups before and after adjustment for age, height weight and sex. Similar results in different DXA, pQCT and pQCT-FE variables were observed between groups when females and males were analysed separately (Suppl. Tables 1 and 2).

Age, height and weight did not exhibit collinearity with each group of DXA, pQCT and pQCT-FE variables in any of the regression models, with all corresponding VIF < 5 (Table 2). Collinearity, however, was identified with other predictors in each. Among DXA variables, the highest VIF was found with TH aBMD (VIF = 5.1). For standard pQCT

Table 1 Characteristics of study participants

	Fracture (<i>n</i> = 108)	Control (<i>n</i> = 120)	<i>p</i>
Age (years, mean ± SD)	68.3 ± 8.2	69.5 ± 8.1	0.27
Height (cm, mean ± SD)	165.6 ± 8.3	166.2 ± 6.3	0.54
Weight (kg, mean ± SD)	74.9 ± 13.7	72.2 ± 12.8	0.13
BMI (kg/m ² , mean ± SD)	27.4 ± 5.2	26.5 ± 4.4	0.16
Sex (female, <i>n</i> , %)	77 (71.3%)	85 (70.8%)	0.94
Radius length (mm, mean ± SD)	229.6 ± 25.2	232.0 ± 27.0	0.49
Tibia length (mm, mean ± SD)	352.1 ± 19.9	355.4 ± 21.1	0.23
Fracture risk factors (<i>n</i> , %)			
Smoking	17 (15.7%)	7 (5.8%)	<i>0.01</i>
Alcohol	15 (13.9%)	11 (9.2%)	0.26
Rheumatoid arthritis	13 (12.0%)	5 (4.2%)	<i>0.03</i>
Parental hip fracture	17 (15.7%)	7 (5.8%)	<i>0.01</i>
Interval between fracture and study visit (days, mean ± SD)	56.6 ± 13.2		
Fracture site ^a			
Radius/ulna	74		
Hand	4		
Humerus	11		
Tibia/fibula	17		
Ankle/foot	6		
Femur	6		
Pelvis	2		
Rib	1		
Spine	1		

^a A total of 13 patients (7 females and 6 males) had fracture of more than one site: 6 females with two fracture sites and 1 female with three fracture sites and 6 males with two fracture sites

p values with statistical significance are in italics

variables, radius tot vBMD (VIF = 11.0) and tibia SSI_p (VIF = 16.0) had the highest collinearity with other standard pQCT variables. Strong collinearity with high VIF values was observed in all groups of pQCT-FE properties, indicating strong correlations among the stiffness estimates of the four loading cases at the same site, especially between k_{comp} and k_{shear} (e.g. at 4% tibia, VIF = 641.8 and 598.6, respectively). Similar trends were observed when females and males were analysed separately (Suppl. Tables 1 and 2).

The ability of each DXA, standard pQCT and pQCT-FE property to classify between fracture and control groups (i.e. OR, specificity, sensitivity and AUROC derived from the logistic regression models) in all participants, and females and males separately, is shown in Table 3. In the pooled analysis, odds of fracture increased 1.53-fold per SD decrease in DXA TH aBMD [95% CI (1.01, 2.15)]. Odds of fracture increased more per SD decrease of tibia Trb vBMD and 4% tibia k_{shear} , which were 7.64 [95% CI (1.92, 26.51)] and 9.13 [95% CI (1.87, 31.36)], respectively. The highest AUROC was observed with 4% tibia k_{shear} , which was 0.79 [95% CI (0.74, 0.84)], compared with 0.69 [95% CI (0.62, 0.75)] for TH aBMD and 0.74 [95% CI (0.68, 0.80)] for tibia Trb vBMD. Specificity and sensitivity were 66.7% and 78.7% for 4% tibia

k_{shear} compared with 76.7% and 54.8% for TH aBMD, respectively. Pairwise comparisons (Fig. 2; Table 4) of AUROC for the three key variables (DXA TH aBMD, tibia Trb vBMD and 4% tibia k_{shear}) showed that the AUROC of k_{shear} was higher than TH aBMD ($p = 0.02$). Difference in AUROC was observed neither between tibia Trb vBMD and TH aBMD nor between 4% tibia k_{shear} and tibia Trb vBMD.

In females, odds of fracture increased 1.52-fold per SD decrease in DXA TH aBMD [95% CI (1.01, 2.16)]. Higher ORs were observed for standard pQCT and pQCT-FE properties, which were greatest for tibial Trb vBMD [OR = 8.15, 95% CI (1.78, 39.72)] and k_{shear} at 4% tibia [OR = 10.34, 95% CI (1.91, 43.98)], respectively. Among all variables, the highest AUROC was found with k_{shear} at 4% tibia, which was 0.83 [95% CI (0.77, 0.89)] compared with 0.72 [95% CI (0.64, 0.79)] for DXA TH aBMD and 0.76 [95% CI (0.68, 0.82)] for tibia Trb vBMD. Specificity and sensitivity for k_{shear} at 4% tibia were 79.2% and 69.4%, compared with 72.4% and 52.7% for DXA TH aBMD, respectively. Pairwise comparisons (Fig. 2; Table 4) of AUROC for the three primary variables (DXA TH aBMD, tibia Trb vBMD and 4% tibia k_{shear}) showed that AUROC of k_{shear} was higher than TH aBMD ($p = 0.02$).

Table 2 Comparison of different properties between the fracture and control groups in all participants. Variance inflation factors (VIFs) were calculated for the properties of each modality. Values are expressed as mean \pm 1.0 SD

	Fracture group ($n = 108$)	Control group ($n = 120$)	p	p_{adj}^a	VIF
DXA properties					
LS aBMD (g/cm^2)	1.00 \pm 0.14	1.04 \pm 0.18	0.06	0.17	2.6
TH aBMD (g/cm^2)	0.90 \pm 0.15	0.95 \pm 0.17	0.02	0.13	5.1
FN aBMD (g/cm^2)	0.75 \pm 0.11	0.77 \pm 0.13	0.21	0.27	5.0
Standard pQCT radius properties					
Tot vBMD (mg/cm^3)	281.75 \pm 61.17	282.46 \pm 55.61	0.93	0.97	11.0
Trb vBMD (mg/cm^3)	164.92 \pm 46.08	182.03 \pm 36.47	< 0.01	0.01	7.3
Trb CSA (mm^2)	178.45 \pm 39.34	187.27 \pm 31.69	0.06	0.11	3.5
Crt vBMD (mg/cm^3)	1123.77 \pm 57.94	1139.88 \pm 49.45	0.02	0.07	5.7
Crt Thk (mm)	2.26 \pm 0.35	2.39 \pm 0.33	< 0.01	0.09	3.9
SSI _p (mm^3)	256.87 \pm 54.54	266.91 \pm 51.24	0.15	0.21	10.8
Standard pQCT tibia properties					
Tot vBMD (mg/cm^3)	264.56 \pm 52.02	278.38 \pm 52.52	0.05	0.22	12.7
Trb vBMD (mg/cm^3)	205.63 \pm 48.20	223.47 \pm 44.13	< 0.01	0.02	6.9
Trb CSA (mm^2)	527.82 \pm 77.57	541.31 \pm 76.32	0.19	0.47	3.7
Crt vBMD (mg/cm^3)	1120.72 \pm 42.38	1129.94 \pm 39.18	0.09	0.14	5.1
Crt Thk (mm)	4.01 \pm 0.80	4.16 \pm 0.68	0.13	0.29	3.9
SSI _p (mm^3)	2248.76 \pm 394.44	2369.36 \pm 397.11	0.02	0.17	16.0
pQCT-FE properties (4% radius)					
k_{comp} (kN/mm)	39.47 \pm 22.23	45.46 \pm 26.79	0.07	0.11	92.1
k_{shear} (kN/mm)	9.92 \pm 5.44	10.92 \pm 6.06	0.19	0.28	107.5
k_{bend} (Nm/deg)	20.99 \pm 12.12	23.51 \pm 14.26	0.15	0.33	18.7
k_{torsion} (Nm/deg)	16.87 \pm 8.83	18.52 \pm 10.97	0.22	0.29	25.1
pQCT-FE properties (66% radius)					
k_{comp} (kN/mm)	196.85 \pm 58.97	221.41 \pm 71.53	< 0.01	0.04	374.2
k_{shear} (kN/mm)	56.61 \pm 17.72	64.10 \pm 17.87	< 0.01	0.07	354.7
k_{bend} (Nm/deg)	36.62 \pm 10.58	48.75 \pm 22.17	< 0.01	0.03	6.9
k_{torsion} (Nm/deg)	28.98 \pm 11.78	32.41 \pm 12.42	0.03	0.06	8.5
pQCT-FE properties (4% tibia)					
k_{comp} (kN/mm)	1017.10 \pm 285.44	1224.70 \pm 345.70	< 0.01	< 0.01	641.8
k_{shear} (kN/mm)	275.12 \pm 88.98	356.84 \pm 106.06	< 0.01	0.01	598.6
k_{bend} (Nm/deg)	1866.48 \pm 713.26	2163.96 \pm 677.60	< 0.01	0.06	11.7
k_{torsion} (Nm/deg)	1251.59 \pm 398.72	1525.70 \pm 481.82	< 0.01	0.05	14.9
pQCT-FE properties (66% tibia)					
k_{comp} (kN/mm)	3402.49 \pm 652.90	3681.22 \pm 648.68	< 0.01	0.03	971.5
k_{shear} (kN/mm)	1015.76 \pm 193.17	1113.30 \pm 197.80	< 0.01	0.04	827.1
k_{bend} (Nm/deg)	2524.93 \pm 1043.97	2768.08 \pm 1143.02	0.02	0.04	5.2
k_{torsion} (Nm/deg)	2461.42 \pm 572.77	2578.14 \pm 563.71	0.12	0.19	5.3

p values with statistical significance are in italics. Age, height and weight were also included in each regression model, and all VIFs for them were lower than 5

^a p values for comparison between groups after adjusted for age, height and weight

No difference in AUROC was observed between tibia Trb vBMD and TH aBMD ($p = 0.4$). There was a trend that AUROC of k_{shear} was higher than that of tibia Trb vBMD with a $p = 0.07$.

For male participants, odds of fracture increased 1.55-fold per SD decrease in DXA TH aBMD [95% CI (1.02, 2.07)].

Higher ORs were observed for standard pQCT and pQCT-FE properties, which were greatest for tibia Trb vBMD [OR = 6.58, 95% CI (2.43, 10.70)] and k_{bend} at 4% tibia [OR = 8.32, 95% CI (4.15, 33.84)], respectively. Among all variables, the highest AUROC was found with k_{bend} at 4% tibia, which was 0.81 [95% CI (0.70, 0.90)] compared with 0.62

Table 3 Odds ratio, specificity, sensitivity and area under receiver operating curve (AUROC) of receiver operative curve derived for key variables

	OR (95% CI)	Specificity (%)	Sensitivity (%)	AUROC (95% CI)
All participants				
LS aBMD	1.26 (1.04, 1.66)	74.1	61.4	0.64 (0.56, 0.74)
TH aBMD	1.53 (1.01, 2.15)	76.7	54.8	0.69 (0.62, 0.75)
FN aBMD	1.19 (0.91, 1.60)	75.0	57.0	0.61 (0.54, 0.69)
Radius Trb vBMD	3.01 (0.92, 4.57)	70.2	61.4	0.70 (0.60, 0.79)
Tibia Trb vBMD	7.64 (1.92, 26.51)	76.7	62.0	0.74 (0.68, 0.80)
k_{bend} (66% radius)	5.84 (0.99, 7.23)	69.7	63.2	0.73 (0.64, 0.80)
k_{shear} (4% tibia)	9.13 (1.87, 31.36)	66.7	78.7	0.79 (0.74, 0.84)
k_{bend} (66% tibia)	5.23 (1.85, 15.37)	74.1	65.8	0.78 (0.70, 0.86)
Females				
LS aBMD	1.23 (1.04, 1.59)	71.0	62.5	0.65 (0.58, 0.74)
TH aBMD	1.52 (1.01, 2.16)	72.4	52.7	0.72 (0.64, 0.79)
FN aBMD	1.15 (0.80, 1.66)	74.5	52.1	0.62 (0.55, 0.70)
Radius Trb vBMD	3.28 (0.89, 4.85)	67.4	62.2	0.70 (0.60, 0.78)
Tibia Trb vBMD	8.15 (1.78, 39.72)	65.9	75.3	0.76 (0.68, 0.82)
k_{bend} (66% radius)	5.95 (0.96, 9.39)	71.2	62.2	0.71 (0.64, 0.77)
k_{shear} (4% tibia)	10.34 (1.91, 43.98)	79.2	69.4	0.83 (0.77, 0.89)
k_{bend} (66% tibia)	6.04 (1.71, 18.51)	74.5	62.2	0.78 (0.70, 0.86)
Males				
LS aBMD	1.49 (1.06, 1.89)	65.7	67.7	0.61 (0.52, 0.71)
TH aBMD	1.55 (1.02, 2.07)	65.7	64.5	0.62 (0.49, 0.74)
FN aBMD	1.21 (0.99, 1.52)	67.7	64.5	0.57 (0.50, 0.66)
Radius Trb vBMD	2.16 (1.02, 3.22)	74.3	77.4	0.73 (0.60, 0.83)
Tibia Trb vBMD	6.58 (2.43, 10.70)	74.3	64.5	0.71 (0.59, 0.82)
k_{bend} (66% radius)	3.27 (2.71, 3.82)	74.2	67.7	0.78 (0.65, 0.89)
k_{bend} (4% tibia)	8.32 (4.15, 33.84)	80.0	74.2	0.81 (0.70, 0.90)
k_{bend} (66% tibia)	4.64 (2.37, 7.09)	65.7	67.7	0.80 (0.72, 0.88)

[95% CI (0.49, 0.74)] for DXA TH aBMD and 0.71 [95% CI (0.59, 0.82)] for tibia Trb vBMD. Specificity and sensitivity for k_{bend} at 4% tibia were 80.0% and 74.2%, compared with 65.7% and 64.5% for DXA TH aBMD, respectively. Pairwise comparisons (Fig. 2; Table 4) found higher AUROC for 4% tibia k_{bend} than for TH aBMD ($p = 0.03$). No difference in AUROC was observed either between standard pQCT and DXA variables or between pQCT-FE and standard pQCT variables.

Discussion

This study evaluated whether pQCT-derived FE modeling provided improved discrimination between non-vertebral, low-trauma fracture patients with predominantly peripheral fractures and age-matched controls. Peripheral QCT scans of the radius and the tibia were performed on patients with recent non-vertebral, low-trauma fracture and age-matched healthy controls. The fracture group consisted primarily of ambulatory care patients with limb fractures; therefore, as expected, they

were relatively young compared with patients presenting with spine and hip fractures. Thus, our pQCT findings are likely to reflect bone fragility at the relevant peripheral sites in this age group. Peripheral QCT can differentiate the cortical and trabecular compartments of bone, which is advantageous as the two types of bone change differently in response to ageing, bone diseases and treatment [24]. In this study, pQCT-FE variables were found to have enhanced diagnostic performance compared with DXA and statistically comparable diagnostic performance with standard pQCT variables. By incorporating the BMDs across these different compartments in FE models, we hypothesized that predictions of bone stiffness may be used to better discriminate between fracture patients and healthy controls compared to DXA.

QCT-based FE modelling has been used in clinical studies to assess bone strength of the proximal femur and spine due to its strong predictive ability for fracture failure load [13, 14]. In the last decade, a dedicated peripheral CT scanner with higher image resolution and voxel size emerged in clinical research. High-resolution pQCT (HR-pQCT) of the latest generation can achieve voxel sizes of 61 μm which enables depiction of

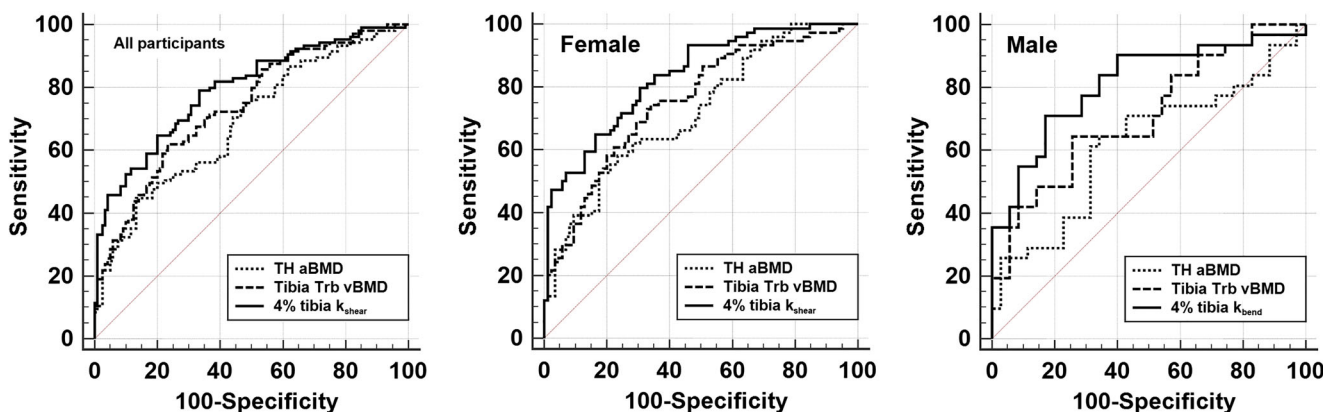


Fig. 2 Comparisons of AUROC of primary variables in all participants, females and males

the microstructure of the radius and the tibia. While micro-FE (μ FE) generated from HR-pQCT images has good ability to discriminate between fracture patients and controls [25] and is associated with fracture occurrence during follow-up [26], there are several drawbacks with this technique when used in clinical settings. It is time-consuming to scan, set up and analyse an FE model for individual patients from HR-pQCT images (3 to 10 h; [27]); hence, it is not efficient for fracture risk screening or diagnosing osteoporosis in a clinical setting. The amount of time required to setup QCT-based FE analysis is similarly problematic. While HR-pQCT scanners expose patients to slightly greater radiation than for pQCT [28], the difference is negligible considering the minimal radiation dose associated with either scanning system. HR-pQCT provides considerably more bone structural information than pQCT. However, HR-pQCT scanners present increased procurement and maintenance costs compared to pQCT, which might restrict their widespread clinical use. Hence, we thought it worthwhile to evaluate the possible role of pQCT in enhancing the recognition of bone fragility in clinical settings. In our experience, pQCT-FE from single cross sections solves each of these issues. Better diagnostic ability than DXA was achieved with simpler set up, thus shorter time to scan patients and to set up individual pQCT-FE models, with lower radiation exposure and cost. As a dedicated tool for the measurement of clinically relevant sites with several practical advantages, pQCT-FE may play a complementary role in future clinical studies assessing bone health.

Significant differences between groups were observed in pQCT-FE properties, especially at the 4% tibia site, and in some standard pQCT properties. While trabecular or cortical vBMD differed statistically between fracture patients and healthy controls, no difference was identified in SSI_p , the bone strength index reported to be a good measure of bone strength and a good predictor for fracture [8]. Fracture odds increased by 10.34 [95% CI (1.91, 43.98)]- and 10.17 [95% CI (1.60, 42.21)]-fold per SD decrease in pQCT-FE properties and were only 1.52 [95% CI (1.01, 2.16)] and 1.74 [95% CI (1.02,

2.37)] with DXA aBMD measures in females and males, respectively. pQCT-FE properties also had higher diagnostic ability than DXA with AUROC of 0.83 vs 0.72 ($p = 0.02$) in females and that of 0.81 vs 0.62 in males. This strength was also with improvement in specificity (79.2% vs 72.4% in females, 80.0% vs 65.6% in males) and sensitivity (69.4% vs 52.7% in females, 74.2% vs 64.5% in males). The pQCT-FE variables with highest AUROC were observed at the 4% tibia site, although the specific loading variable differed between females (k_{shear}) and males (k_{bend}). However, since pQCT-FE variables at the same site had high VIFs thus correlated strongly with each other, the difference was not considered to imply different mechanical performance between females and males. Overall, pQCT-FE models improved clinical performance in the identification of patients with increased fracture risk compared with DXA.

The best fracture discrimination was observed for pQCT-FE variables at the trabecular-rich site in the tibia. It should be noted that while pQCT-FE variables are computed from both trabecular and cortical bone, their relative contributions will depend on the site; hence, the pQCT-FE variables at the distal site will be more influenced by trabecular bone than at the proximal site. Since the pQCT-FE variables provided the greatest fracture discrimination at the distal tibia, the trabecular bone should be considered of greater importance for classification of peripheral appendicular fractures.

Among the standard pQCT and pQCT-FE variables, better performance was generally observed for variables obtained at the tibia compared to the radius. At the 4% tibia site, all pQCT-FE properties differed significantly between groups with the highest OR for fracture and highest AUROC to classify fracture patients from healthy controls. This finding contrasts with peripheral clinical fracture locations, where more fractures occur at the distal radius compared to the distal tibia. Many studies utilizing DXA have confirmed that scans of one specific site predict fracture of that site better than scans of other sites do. The finding from the current study is unexpected considering most fractures were forearm fractures. However, we do note

Table 4 Pairwise comparison of AUROC of primary variables in females and males

	Mean difference	95% CI	<i>p</i>
All participants			
Tibia Trb vBMD—TH aBMD	0.05	(− 0.03, 0.13)	0.21
<i>k_{shear}</i> 4% tibia—TH aBMD	0.11	(0.02, 0.20)	<i>0.02</i>
<i>k_{shear}</i> 4% tibia—Tibia Trb vBMD	0.05	(− 0.03, 0.14)	0.19
Females			
Tibia Trb vBMD—TH aBMD	0.03	(− 0.05, 0.12)	0.42
<i>k_{shear}</i> 4% tibia—TH aBMD	0.11	(0.02, 0.21)	<i>0.02</i>
<i>k_{shear}</i> 4% tibia—Tibia Trb vBMD	0.08	(− 0.01, 0.17)	0.07
Male			
Tibia Trb vBMD—TH aBMD	0.09	(− 0.09, 0.27)	0.32
<i>k_{bend}</i> 4% tibia—TH aBMD	0.19	(0.02, 0.36)	<i>0.03</i>
<i>k_{bend}</i> 4% tibia—Tibia Trb vBMD	0.10	(− 0.06, 0.26)	0.21

p values with statistical significance are in italics

similar findings by Sornay-Rendu et al [11] utilizing HR-pQCT between patients with mixed fractures and controls. In their study, none of the radius variables differed between groups after adjustment for radius aBMD, while several tibia variables remained statistically significant including both total and trabecular density at the distal tibia, cortical thickness and trabecular thickness. Furthermore, OR per SD decrease were also higher for tibia variables than for radius variables in this study. This may be due to variations in radius morphology and bone density across the population [29], which makes this site less sensitive to identify a fracture risk threshold. Indeed, we noticed higher coefficients of variance in radius variables than in the tibia from previous studies conducted at different centres using pQCT [30–32] or HR-pQCT [33–35], especially variables at distal site. Another possibility is that movement of the radius due to breathing and upper body movement may have affected imaging at this site to a greater degree than the distal tibia. The controls may have represented a more physically active cohort compared to the fracture patients, which may have contributed to greater bone density, particularly at the tibia, and a better preservation of balance thus reducing their risk of falls and fracture [36]. In addition, it may also result from the mixed fracture types in the studied population. However, even in patients with distal radius fracture only, pQCT-measured tibia variables still seem to have comparable ability to discriminate between fractures and controls [10].

A key limitation in the FE models was that the loading and boundary conditions in the simulations were artificial compared to daily loading of the radius and the tibia in vivo, where a loading combination of all cases occurs simultaneously [37]. The logic for adopting these loading cases in the pQCT-FE models is that a bone's strength is proportional to its weakest resistance for an idealised loading condition. Indeed, this assumption has been adopted extensively in HR-pQCT-based μ FE models where idealised axial compression was used to

assess fracture risk [38]. Nevertheless, these idealized loading conditions when combined with the thin cross-sectional geometry of the FE models would have led to bone stiffness predictions that differed from those encountered in vivo. Hence, the bone stiffnesses predicted in the current study are only proportional to whole bone fracture load applicable for comparing relative differences between cohorts of patients rather than assessing the absolute stiffness of bone for an individual.

pQCT has an inferior spatial resolution compared to HR-pQCT, thus provides limited information about bone microstructure. This limitation of pQCT might restrict its wide research utility where knowledge of microstructure is required. However, comparable AUROC was reported in studies investigating the diagnostic ability of HR-pQCT and μ FE in distinguishing controls from either patient with radius fracture [39] or with mixed low-trauma fractures [40]. The degree to which HR-pQCT and μ FE can improve the diagnostic performance directly compared with pQCT-FE in identifying fracture patients is still uncertain. Future studies are needed to confirm whether comparable diagnostic ability can be achieved using the relatively low-resolution pQCT scanner considering its lower procurement and maintenance costs.

Due to lack of thoracolumbar X-ray/vertebral fracture assessment, there is still a possibility that a sub-group of controls had asymptomatic vertebral fracture. We acknowledge that this is a limitation of the study and might reduce rather than exaggerate the apparent differences in FEM measures between fracture and non-fracture individuals. It is estimated that nearly 70% of vertebral fractures are missed in community in clinical practice [41]. While improving diagnosis rate of asymptomatic vertebral fracture remains difficult, we do notice that osteoporotic vertebral fracture is more prevalent for ages greater than those seen in the current study [42]. In addition, recruiting strategies were applied to eliminate the impact of vertebral fracture as much as possible. Subjects were screened for symptoms such

as chronic back pain or loss of height on a self-reported questionnaire. As a proportion of vertebral fractures result from prolonged use of glucocorticoid agents, “currently taking or have recently taken glucocorticoid agents” was one of the general exclusion criteria for both groups.

DXA measurements of the forearm were not available in this study. DXA measurement of the one-third radius predicts wrist fracture better than central DXA measurements; therefore, the subsequent inability to relate pQCT and pQCT-FE to DXA values at similar anatomic site is another limitation of this study, especially for the reported population in whom a majority had forearm fractures. However, the ability of both distal radius and central DXA to predict all types of fragility fracture is comparable [43]. The study by Amiri et al [44] reported good linear correlation between radius and central DXA results, which suggests that the trends in the central DXA results would remain similar if radius DXA measurements were used. The aim of the current study was to compare the pQCT-FE method with the most-accepted DXA measurements used for osteoporosis and fracture risk assessment in clinical practice, which both the WHO and ISCD recommend as central DXA. However, inclusion of radius DXA measurements and their comparisons to pQCT and pQCT-FE measures would provide additional information on the application of this novel yet simple technology and would be of added research interest.

In summary, pQCT-based FE models were applied together with standard pQCT and DXA properties to distinguish patients with recent non-vertebral fragility fracture from healthy controls. Improved diagnostic ability was observed for pQCT-FE, but not primary pQCT variables, compared with DXA properties in both females and males, although no statistical difference was observed in AUROC between primary pQCT and pQCT-FE variables. These results may provide an enhanced assessment for bone fragility in clinical settings considering the limitations of DXA, which is the most established modality currently. This study also strongly supports the rationale for future longitudinal studies with follow-up data for fracture risk assessment using pQCT-FE analysis. Recognizing and quantifying bone fragility before a major osteoporotic fracture occurs may bring considerable clinical benefits. Therefore, the potential clinical impact of applying this technology warrants exploration.

Acknowledgements The authors would like to thank all subjects for their participation in this study and the University of the Third Age for providing assistance in participant recruitment. We acknowledge Dr Ashwini Kale for performing DXA and pQCT scans, Mr Richard Farrugia for coordinating the fracture liaison service from which all fracture patients were recruited and Associate Professor Andrew Bucknill for his strong support of recruitment at the fracture liaison service.

Funding information HJ is funded with a joint PhD scholarship by China Scholarship Council (funding reference: CSC201608240003) and the University of Melbourne.

Compliance with ethical standards

Verbal and written informed consents were obtained from each participant after they were provided with detailed information about the study. This study was approved by Melbourne Health Human Research Ethics Committee (ethics approval number MH 2014.143).

Conflicts of interest None.

References

1. Wright NC, Looker AC, Saag KG, Curtis JR, Delzell ES, Randall S, Dawson-Hughes B (2014) The recent prevalence of osteoporosis and low bone mass in the United States based on bone mineral density at the femoral neck or lumbar spine. *J Bone Miner Res* 29(11):2520–2526
2. Hernlund E, Svedbom A, Ivergard M, Compston J, Cooper C, Stenmark J, McCloskey EV, Jonsson B, Kanis JA (2013) Osteoporosis in the European Union: medical management, epidemiology and economic burden. A report prepared in collaboration with the International Osteoporosis Foundation (IOF) and the European Federation of Pharmaceutical Industry Association (EFPIA). *Arch Osteoporos* 8(1-2):136
3. Cauley JA (2017) Osteoporosis: fracture epidemiology update 2016. *Curr Opin Rheumatol* 29(2):150–156
4. Jiang H, Yates CJ, Gorelik A, Kale A, Song Q, Wark JD (2018) Peripheral quantitative computed tomography (pQCT) measures contribute to the understanding of bone fragility in older patients with low-trauma fracture. *J Clin Densitom* 21(1):140–147
5. Fonseca H, Moreira-Goncalves D, Vaz M, Fernandes MH, Ferreira R, Amado F, Mota MP, Duarte JA (2012) Changes in proximal femur bone properties following ovariectomy and their association with resistance of fracture. *J Bone Miner Res* 30(3):282–292
6. Haentjens P, Johnell O, Kanis JA, Bouillon R, Cooper C, Lamraski G, Vanderschueren D, Kaufman JM, Boonen S, Network on Male Osteoporosis in Europe (NEMO) (2004) Evidence from data searches and life-table analyses for gender-related differences in absolute risk of hip fracture after Colles’ or spine fracture: Colles’ fracture as an early and sensitive marker of skeletal fragility in white men. *J Bone Miner Res* 19(12):1933–1944
7. Muller ME, Webber CE, Bouxsein ML (2003) Predicting the failure load of the distal radius. *Osteoporos Int* 14(4):345–352
8. Kontulainen SA, Johnston JD, Liu D, Leung C, Oxland TR, McKay HA (2008) Strength indices from pQCT imaging predict up to 85% of variance in bone failure properties at tibial epiphysis and diaphysis. *J Musculoskelet Nueronal Interact* 8(4):401–409
9. Weatherholt AM, Avin KG, Hurd AL, Cox JL, Marberry ST, Santoni BG, Warden SJ (2015) Peripheral quantitative computed tomography predicts humeral diaphysis torsional mechanical properties with good short-term precision. *J Clin Densitom* 18(4):551–559
10. Crockett C, Arnold CM, Farthing JP, Chilibeck PD, Johnston JD, Bath B, Baxter-Jones ADG, Kontulainen SA (2015) Bone strength and muscle properties in postmenopausal women with and without a recent distal radius fracture. *Osteoporos Int* 26(10):2461–2469
11. Sornay-Rendu E, Boutroy S, Munoz F, Delmas PD (2007) Alterations of cortical and trabecular architecture are associated with fractures in postmenopausal women, partially independent of decreased BMD measured by DXA: the OFELY study. *J Bone Miner Res* 22(3):425–433
12. Sheu Y, Zmuda JM, Boudreau RM, Petit MA, Ensrud KE, Bauer DC, Gordon CL, Orwoll ES, Cauley JA; Osteoporotic Fractures in

- Men MrOS Research Group (2011) Bone strength measured by peripheral quantitative computed tomography and the risk of nonvertebral fractures: the osteoporotic fractures in men (MrOS) study. *J Bone Miner Res* 26(1):63–71
13. Dall'ara E, Schmidt R, Pahr D, Varga P, Chevalier Y, Patsch J, Kainberger F, Zysset P (2010) A nonlinear finite element model validation study based on a novel experimental technique for inducing anterior wedge-shape fractures in human vertebral bodies in vitro. *J Biomech* 43(12):2374–2380
 14. Nishiyama KK, Gilchrist S, Guy P, Crompton P, Boyd SK (2013) Proximal femur bone strength estimated by a computationally fast finite element analysis in a sideways fall configuration. *J Biomech* 46(7):1231–1236
 15. Cody DD, Gross GJ, Hou FJ, Spencer HJ, Goldstein SA, Fyhrie DP (1999) Femoral strength is better predicted by finite element models than QCT and DXA. *J Biomech* 32(10):1013–1020
 16. Ulrich D, van Rietbergen B, Laib A, Rueggsegger P (1999) Load transfer of the distal radius from in-vivo high-resolution CT-imaging. *J Biomech* 32(8):821–828
 17. Gray HA, Taddei F, Zavatsky AB, Cristofolini L, Gill HS (2008) Experimental validation of a finite element model of a human cadaveric tibia. *J Biomech Eng* 130(3):031016
 18. Edwards WB, Troy KL (2012) Finite element prediction of surface strain and fracture strength at the distal radius. *Med Eng Phys* 34(3):290–298
 19. Yates CJ, Chauchard MA, Liew D, Bucknill A, Wark JD (2015) Bridging the osteoporosis treatment gap: performance and cost-effectiveness of a fracture liaison service. *J Clin Densitom* 18(2):150–156
 20. Robinson DL, Jiang H, Song Q, Yates C, Lee PVS, Wark JD (2019) The application of finite element modelling based on clinical pQCT for classification of fracture status. *Biomech Model Mechanobiol* 18(1):245–260
 21. Morgan EF, Bayraktar HH, Keaveny TM (2003) Trabecular bone modulus-density relationships depend on anatomic site. *J Biomech* 36(7):894–904
 22. Ringle CM, Wende S, Becker J-M. SmartPLS 3. Boenningstedt SmartPLS GmbH. www.smartpls.com. Accessed 24 Jan 2019
 23. DeLong ER, Delong DM, Clarke-Pearson DL (1988) Comparing the areas under two or correlated receiver operating characteristics curves: a nonparametric approach. *Biometrics* 44(3):837–845
 24. Clarke B (2008) Normal bone anatomy and physiology. *Clin J Am Soc Nephrol* 3(Suppl 3):S131–S139
 25. Boutroy S, van Rietbergen B, Sornay-Rendu E, Munoz F, Bouxsein M, Delmas PD (2008) Finite element analysis based on in vivo HR-pQCT images of the distal radius is associated with wrist fracture in postmenopausal women. *J Bone Miner Res* 23(3):392–399
 26. Sornay-Rendu E, Boutroy S, Duboeuf F, Chapurlat RD (2017) Bone microarchitecture assessed by HR-pQCT as predictor of fracture risk in postmenopausal women: the OFELY Study. *J Bone Miner Res* 32(6):1243–1251
 27. Kawalilak CE, Kontulainen SA, Amini MA, Lanovaz JL, Olszynski WP, Johnston JD (2016) In vivo precision of three HR-pQCT-derived finite element models of the distal radius and tibia in postmenopausal women. *BMC Musculoskelet Disord* 17(1):1–11
 28. Stagi S, Cavalli L, Cavalli T, de Martino M, Brandi ML (2016) Peripheral quantitative computed tomography (pQCT) for the assessment of bone strength in most of bone affecting conditions in developmental age: a review. *Ital J Pediatr* 42:88
 29. Boyd SK (2008) Site-specific variation of bone micro-architecture in the distal radius and tibia. *J Clin Densitom* 11(3):424–430
 30. Reina P, Cointy GR, Nociolino L, Feldman S, Ferretti JL, Rittweger J, Capozza RF (2015) Analysis of the independent power of age-related, anthropometric and mechanical factors as determinants of the structure of radius and tibia in normal adults. A pQCT study. *J Musculoskelet Nueronal Interact* 15(1):10–22
 31. Van Caenegem E, Taes Y, Wierckx K, Vandewalle S, Toye K, Kaufman J-M, Schreiner T, Haraldsen I, T'Sjoen G (2013) Low bone mass is prevalent in male-to-female transsexual person before the start of cross-sex hormonal therapy and gonadectomy. *Bone* 54(1):92–97
 32. Saarnio E, Pekkinen M, Itkonen ST, Kemi V, Karp H, Ivaska KK, Risteli J, Koivula M-K, Karkkainen M, Makitie O, Sievanen H, Lamberg-Allardt C (2018) Low free 25-hydroxyvitamin D and high vitamin D binding protein and parathyroid hormone in obese Caucasians. A complex association with bone? *PLoS One* 13(2)
 33. Marques IDB, Araujo MJCLN, Gracioli FG, dos Reis LM, Pereira RM, Custodio MR, Jorgetti V, Elias RM, David-Neto E, Moyses RMA (2017) Biopsy vs. peripheral computed tomography to assess bone disease in CKD patients on dialysis: differences and similarities. *Osteoporos Int* 28(5):1675–1683
 34. Schafer AL, Burghardt AJ, Sellmeyer DE, Palermo L, Shoback DM, Majumdar S, Black DM (2013) Postmenopausal women treated with combination parathyroid hormone (1-84) and ibandronate different microstructural changes at the radius vs. tibia: the PTH and Ibandronate Combination Study (PICS). *Osteoporos Int* 24(10):2591–2601
 35. Zanchetta MB, Costa F, Longobardi V, Longarini G, Mazure RM, Moreno ML, Vazquez H, Silveira F, Niveloni S, Smecuol E, de la Paz TM, Hwang HJ, Gonzalez A, Maurino EC, Bogado C, Zanchetta JR, Bai JC (2015) Significant bone microarchitecture impairment in premenopausal women with active celiac disease. *Bone* 76:149–157
 36. Famula A, Nowotny-Czupryna O, Czupryna K, Nowotny J (2013) Previous physical activity and body balance in elderly people. *Biol Sport* 30(4):311–315
 37. Yang PF, Sanno M, Ganse B, Koy T, Bruggemann GP, Muller LP, Rittweger J (2014) Torsion and antero-posterior bending in the in vivo human tibia loading regimes during walking and running. *PLoS One* 9(4):e94525
 38. Vilayphiou N, Boutroy S, Szulc P, van Rietbergen B, Munoz F, Delmas PD, Chapurlat R (2011) Finite element analysis performed on radius and tibia HR-pQCT images and fragility fractures at all site in men. *J Bone Miner Res* 26(5):965–973
 39. Nishiyama KK, Macdonald HM, Hanley DA, Boyd SK (2013) Women with previous fragility fractures can be classified based on bone microarchitecture and finite element analysis measured with HR-pQCT. *Osteoporos Int* 24:1733–1740
 40. Bielez B, Patsch JM, Fischer L, Bojic M, Winnicki W, Weber M, Cejka D (2017) Cortical porosity not superior to conventional densitometry in identifying hemodialysis patients with fragility fracture. *PLoS One* 12(2):e0171873
 41. Papaioannou A, Watts NB, Kendler DL, Yuen CK, Adachi JD, Ferko N (2002) Diagnosis and management of vertebral fractures in elderly adults. *Am J Med* 113(3):220–228
 42. Van Staa TP, Dennison EM, Leufkens HG, Cooper C (2001) Epidemiology of fractures in England and Wales. *Bone* 29(6):517–522
 43. Stone KL, Seeley DG, Lui LY, Cauley JA, Ensrud K, Browner WS, Nevitt MC (2003) Cummings SR; Osteoporotic Fractures Research Group. BMD at multiple sites and risk of fracture of multiple types: long-term results from the Study of Osteoporotic Fractures. *J Bone Miner Res* 18(11):1947–1954
 44. Amiri L, Kheiltash A, Movassaghi S, Moghaddassi M, Seddigh L (2017) Comparison of bone density of distal radius with hip and spine using DXA. *Acta Med Iran* 55(2):92–96